Soil prokaryotic communities in Chernobyl waste disposal trench T22 are modulated by organic matter and radionuclide contamination

Nicolas Theodorakopoulos, Laureline Fevrier, mohamed Barakat, Philippe Ortet, Richard Christen, Laurie Piette, Sviatoslav Levchuk, Karine Beaugelin-Seiller, Claire Sergeant, C. Berthomieu, et al.

OXFORD UNIVERSITY PRESS | FEMS Microbiology Ecology

http://mc.manuscriptcentral.com/fems

Soil prokaryotic communities in Chernobyl waste disposal trench T22 are modulated by organic matter and radionuclide contamination.

Journal:	*FEMS Microbiology Ecology*
Manuscript ID	FEMSEC-17-03-0144.R1
Manuscript Type:	Research article
Date Submitted by the Author:	23-May-2017
Complete List of Authors:	Theodorakopoulos, Nicolas; IRSN, SERIS/L2BT Fevrier, Laureline; Institut de Radioprotection et de Surete Nucleaire Cadarache, PRP-ENV,SERIS,L2BT Barakat, Mohamed; CNRS, IBEB Ortet, Philippe; CEA, IBEB Christen, Richard; CNRS, UMR7138 Piette, Laurie; CEA, DSV/SBVME/LIPM Levchuk, Sviatoslav; UIAR, NUBiP Beaugelin-Seiller, Karine; Institut de Radioprotection et de Surete Nucleaire Cadarache, PRP-ENV, SERIS, LRTE sergeant, Claire; Centre d\'etudes nucleaires de Bordeaux Gradignan, UMR5797 Berthomieu, Catherine; CEA, DRF/SBVME/LIPM Chapon, Virginie; CEA, DRF/SBVME/LIPM
Keywords:	bacterial diversity, Chernobyl, radionuclide, pyrosequencing

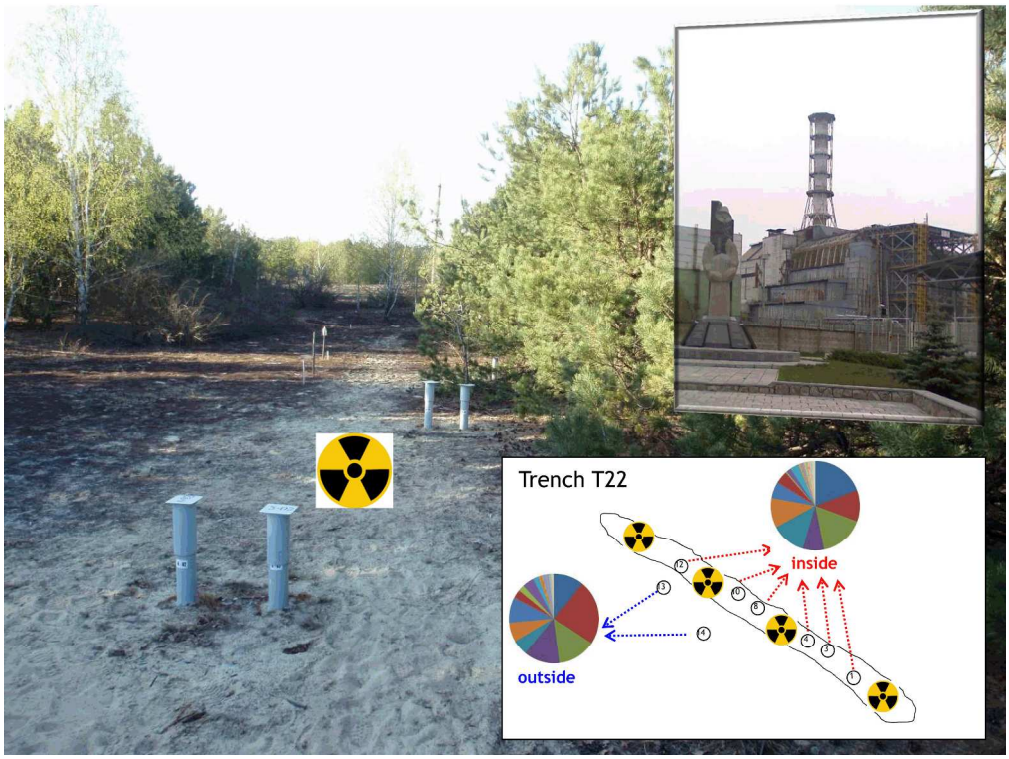

1249x937mm (72 x 72 DPI)

Soil prokaryotic communities in Chernobyl waste disposal trench T22 are modulated by organic matter and radionuclide contamination.

Nicolas Theodorakopoulos[1,2], Laureline Février[2], Mohamed Barakat[3], Philippe Ortet[3], Richard Christen[4,5], Laurie Piette[1], Sviatoslav Levchuk[6], Karine Beaugelin-Seiller[7], Claire Sergeant[8,9], Catherine Berthomieu[1] and Virginie Chapon[1*].

[1] CEA, CNRS, Aix-Marseille Université, UMR 7265 Biologie Végétale et Microbiologie Environnementale, LIPM, 13108 Saint-Paul-lez-Durance, France.

[2] IRSN, PRP-ENV, SERIS, L2BT, 13115 Saint Paul-lez-Durance, France.

[3] CEA, CNRS, Aix-Marseille Université, UMR 7265 Biologie Végétale et Microbiologie Environnementale, LEMIRE, 13108 Saint-Paul-lez-Durance, France.

[4] Université de Nice-Sophia Antipolis, UMR 7138, Systématique, Adaptation, Evolution, Parc Valrose, BP71, 06108 Nice cedex 02, France.

[5] CNRS, UMR 7138, Systématique, Adaptation, Evolution, Parc Valrose, BP71, 06108 Nice cedex 02, France.

[6] Ukrainian Institute of Agricultural Radiology UIAR NUBiP of Ukraine, Mashinobudivnykiv str. 7, Chabany, Kyiv-Svjatoshin Distr, Kyiv Reg., 08162, Ukraine.

[7] IRSN, PRP-ENV, SERIS, LRTE, 13115 Saint Paul-lez-Durance, France.

[8] Université de Bordeaux, CENBG, UMR5797, 33170 Gradignan, France.

[9] CNRS, IN2P3, CENBG, UMR5797, 33170 Gradignan, France.

Running title: Prokaryotic diversity in Chernobyl soils

[*] Corresponding author: Virginie Chapon, CEA, CNRS, Aix-Marseille Université, UMR 7265, LIPM, Bât 185, CEA Cadarache, 13108 Saint-Paul-lez-Durance, France. E-mail: virginie.chapon@cea.fr; Tel. +33442253478; Fax. +33442252625.

Abstract

After the Chernobyl nuclear power plant accident in 1986, contaminated soils, vegetation from the Red Forest, and other radioactive debris were buried within trenches. In this area, trench T22 has long been a pilot site for the study of radionuclide migration in soil. Here, we used 454 pyrosequencing of 16S rRNA genes to obtain a comprehensive view of the bacterial and archaeal diversity in soils collected inside and in the vicinity of the trench T22 and to investigate the impact of radioactive waste disposal on prokaryotic communities. A remarkably high abundance of *Chloroflexi* and AD3 was detected in all soil samples from this area. Our statistical analysis revealed profound changes in community composition at the phylum and OTUs levels and higher diversity in the trench soils as compared to the outside. Our results demonstrate that the total absorbed dose rate by cell and, to a lesser extent the organic matter content of the trench, are the principal variables influencing prokaryotic assemblages. We identified specific phylotypes affiliated to the phyla *Crenarchaeota, Acidobacteria,* AD3, *Chloroflexi, Proteobacteria*, *Verrucomicrobia* and WPS-2, which were unique for the trench soils.

Introduction

In the past decade, uranium mining, military activities and nuclear power plant accidents have introduced anthropogenic radioactive contaminants into the environment (Hu 2008). The Chernobyl nuclear power plant disaster led to the release of 13 650x10^{18} Becquerel (Bq) (Martin-Garin *et al* 2012) and contributed significantly to the dispersal of many radioactive isotopes in the environment such as ^{137}Cs, ^{90}Sr, ^{60}Co, ^{154}Eu, ^{241}Am, ^{234,235,236}U and ^{239,240,241}Pu, exhibiting different kinds of radiation (some are pure α emitters whereas others emit β– and/or γ–radiation). Due to their intrinsic properties (*i.e.* radioactive decay half-life, volatility and mobility), most of these radionuclides (RNs) are highly

persistent in the terrestrial environment. Radiations emitted by RNs present either in the environment or accumulated inside organisms are able to ionize atoms or molecules, with potential consequent damage to living cells. Level of such biological detriment is linked to the energy deposited into organisms exposed to ionizing radiation, under the consensual assumption of additive effects. Thirty years after the accident, ^{137}Cs is the main contributor to the current ambient external gamma dose rate in the Chernobyl exclusion zone. However the proper assessment of the intensity of radiological exposure leading to observed effects requires to consider not only the ambient external dose rates (as often reported in most studies), but the total dose rates to which living organisms are exposed by including all exposure pathways and all RNs whatever their emission types (Garnier-Laplace *et al* 2015).

Soil microorganisms and RNs display complex relationships with each other. On the one hand, bacteria can interact with RNs *via* multiple mechanisms including bioreduction, biomineralization, bioaccumulation or biosorption (Lloyd and Macaskie 2002; Merroun and Selenska-Pobell 2008; Newsome, Morris and Lloyd 2014; Theodorakopoulos *et al* 2015). On the other hand, RNs may exert radio- and chemo-toxic effects on bacteria, thus influencing the structure and activity of microbial communities. Many previous studies have explored the molecular diversity of bacterial communities in various natural or contaminated sites containing radionuclides such as uranium (Selenska-Pobell *et al.* 2001; Rastogi *et al.* 2010; Islam and Sar 2011; Kumar *et al.* 2013; Radeva *et al.* 2013; Yan, Luo and Zhao 2016), uranium and ^{99}Tc (Fields *et al.* 2005; Akob, Mills and Kostka 2007; Barns *et al.* 2007; Waldron *et al.* 2009) and ^{137}Cs and ^{99}Tc (Fredrickson *et al.* 2004). Diverse and complex bacterial assemblages have been evidenced in these habitats and although site-specific composition of bacterial communities is observed, *Proteobacteria* and *Acidobacteria* are frequently well-represented. Several studies highlighted significant changes of bacterial communities upon RNs exposure (Geissler and Selenska-Pobell 2005; Akob, Mills and

Kostka 2007, Rastogi *et al.* 2010; Mondani *et al.* 2011, Islam, Paul and Sar. 2014, Yan, Luo and Zhao 2016).

In the case of Chernobyl, very few studies have been performed, most of which were based on cultivation approaches. These studies have shown a decrease in bacterial diversity under conditions of radioactive contamination/irradiation (Romanovskaya *et al.* 1998, 1999; Romanovskaya, Rokitko and Malashenko 2000; Zavilgelsky *et al.* 1998; Czirják *et al.* 2010). In 2011, the first study based on molecular approaches of sunlight-adapted biofilm microbial communities exposed to different ambient radiation levels (0.35 – 25 μSv/h) was reported from the Chernobyl area (Ragon *et al.* 2011). Although the diversity was similar in irradiated and non-irradiated UV-adapted communities, an increase in the mutation level within some Operational Taxonomic Units (OTUs) was correlated with ambient radiation. Niedrée *et al.* (2013) revealed a shift in bacterial population in soil microcosms upon three-month exposure to Chernobyl-like contamination with ^{90}Sr and ^{137}Cs.

Atmospheric fallout from the CNPP accident resulted in radioactive contamination of large regions. One of the most impacted areas, located in the immediate vicinity of the nuclear power plant, is the so-called Red Forest where the pine trees died upon exposure to extreme radiation doses. Shortly after the CNPP accident, clean-up wastes from the Red Forest and other radioactively contaminated debris were buried in a large network of trenches near the CNPP, leading to highly contaminated environmental locations. After the clean-up operations, the trenches were covered with a thick layer of sand and planted with pine saplings, which are now reclaiming the area. One of these trenches (trench T22) has been studied since 1999, as a model of RN migration in the environment (Martin-Garin 2012). In our previous study (Chapon *et al.* 2012), we identified the presence of complex bacterial communities in contaminated soil and control samples from this site using a community fingerprint method

(DGGE). However, this method did not reveal any dominant community fingerprint related to RN content.

The goals of the present study were to explore composition and diversity of soil prokaryotic communities in this understudied environment and to characterize the impact of the trench conditions (RN contamination and high organic matter content) on these communities. We hypothesized that soil prokaryotic communities inside and outside of trench T22 would differ, in particular upon radiation exposure. Therefore, we used high-throughput pyrosequencing of 16S rRNA genes to compare the prokaryotic communities in soil samples exhibiting contrasted RN contamination levels, collected inside and in the vicinity of the trench T22.

Materials and Methods

Sample collection, isolation of culturable bacteria and DNA extraction

Sampling, soil analyses, isolation of culturable bacteria and DNA extraction procedures were previously described (Chapon *et al.* 2012). Briefly, sandy soil samples containing various RN contents were collected between 50 – 60 cm depth from nine different positions in the area of the RN-contaminated trench T22, located in the Chernobyl exclusion zone (51°23'N,30°04'E; Bugai *et al.* 2005). In April and October 2009, RN-contaminated soil samples (numbers 1, 3, 4, 8, 10 and 12) were collected inside the trench, along with low-contamination controls (numbers 13, 14 and 20) collected in the vicinity (Figure 1). The soil samples were processed at Chernobyl within 18 hours after sampling. In April, environmental DNA was extracted from a single subsample of each soil sample, whereas in October environmental DNA was extracted from triplicate subsamples (designated as a, b and c), after homogenization of the soil. DNA was typically extracted from 1g of soil using the PowerSoil™ DNA isolation kit (MO Bio; USA) and stored at -20°C. Culturable bacteria were

recovered from soil samples in aerobic conditions on non-selective media agar plates (tryptic soy broth and AEM1 medium, see Chapon *et al* 2012).

PCR amplification and pyrosequencing

For the pyrosequencing analyses, amplicons from the V4 region of the 16S rRNA genes were generated by PCR using the universal primer set 530f (5'-GTGCCAGCMGCNGCGG-3'; Dowd *et al.* 2008) and 802r (5'-TACNVGGGTATCTAATCC-3'; Claesson *et al.* 2009). The coverage of this primer set was 89.1% for Bacteria and 54.1% for Archaea with no mismatch and reached 96.8% for Bacteria and 96.5% for Archaea with 2 mismatches as predicted with the Testprime tool of SILVA (Klindworth *et al.* 2013). PCR amplifications were performed in triplicate in 50-µl reactions consisting of: 30 – 50 ng of template DNA, 0.6 µM of forward and reverse primers, 0.2 mM dNTPs, 2 mM $MgCl_2$, 1.25 U of Go Taq® Hot start polymerase (Promega; USA), and 1 X reaction buffer. For PCR, the thermocycler was programmed for an initial denaturation at 94°C for 5 min followed by 30 cycles of amplification (94°C for 30 s, 55°C for 30 s, and 72°C for 45 s) and a final extension at 72°C for 5 min. Triplicate samples were pooled before purification of the amplicons. DNA from each amplicon (500 ng) was sent separately for sequencing by GATC (Konstanz, Germany) using a Roche 454 GS-FLX system (Titanium Chemistry). An adaptor and sample-specific 4-bp Molecular Identifier tag (MID) were added to each amplicon by an additional PCR step before mixing and pyrosequencing. Raw reads are available at the NCBI Sequence Read Archive (accession number PRJNA241298).

Processing of pyrosequencing data

The raw dataset (.sff files from two half-plates) contained 825 622 reads and was analyzed with QIIME version 1.8 (Caporaso *et al.* 2010a) with standard parameters. Overall sequences

with quality score average < 25, short sequences (< 200 bp) and sequences containing mismatches as well as homopolymers were removed. We conducted a denoising of chimeras and the multiplex reads were assigned to corresponding sample according to their barcode, and we carried out Operational Taxonomic Unit (OTU) picking with Uclust (Edgar, 2010). Representative sequences of the OTUs were aligned using the PyNAST algorithm with a minimum percent of 80% (Caporaso *et al*. 2010b). These OTUs were taxonomically classified using RDP method (Wang 2007) and Greengenes database (DeSantis *et al*. 2006). The taxonomic position of bacteria and archaea was characterized using taxa summary QIIME scripts until genus level (L6). Alpha diversity parameters (number of observed OTUs, qualitative Chao1 index, Faith's Phylogenetic Diversity (PD_whole) and Shannon index) were calculated with a fixed number of 16 182 randomly picked reads for each sample. Beta-diversity was calculated using Bray-Curtis and unweighted and weighted UniFrac metrics (Lozupone, 2005). PCoA plots were visualized with Emperor (Vazquez-Baeza, 2013).

The representation of cultured bacteria (described in Chapon *et al.* 2012) in the soil bacterial community was assessed by clustering the 16S sequences derived from these bacteria and the 454 reads in OTUs at 97% sequence similarity.

Analysis of soil physico-chemical parameters

For both sampling dates, pH, water content (WC) and NaOH-extractable organic carbon ($C_{org(NaOH)}$) were analyzed as described in Chapon *et al.* (2012). Briefly, soil pH was measured in a 1:5 soil:water suspension, and 2 g of soil were mixed with 10 mL of distilled water and shaken for 30 min. The pH was measured after decanting and 2 hours of atmosphere equilibration. WC was determined by drying 10 g of soil at 105°C for 24 h. $C_{org(NaOH)}$ was determined by dissolving 0.15 g of soil samples in 1.5 mL of 0.1 M NaOH for 15 h. After decanting and centrifugation, the organic carbon concentration in the supernatant

was determined by spectrometry (absorbance measurement at 280 nm).

The ^{137}Cs concentrations in the soil samples were measured by gamma spectrometry. In addition, ^{241}Am, ^{154}Eu and ^{60}Co concentrations were measured in October 2009 by gamma spectrometry, whereas actinide concentrations (^{234}U, ^{235}U, ^{236}U, ^{232}Th, ^{239}Pu, ^{240}Pu and ^{241}Pu) were measured in April 2009 by ICP-MS after dry "ashing" and mineralization of the soil samples (Chapon *et al.* 2012). ^{90}Sr concentrations were derived from ^{137}Cs content assuming a constant ratio of 1.87 between ^{137}Cs and ^{90}Sr concentrations (Kashparov *et al.* 2001). All RN contents were significantly correlated with ^{137}Cs content (Figure S1) except ^{232}Th whose concentration is unvarying close to its natural value in soil (Table S1). Thus, constant ratios between ^{137}Cs and each RN were used to derive the concentrations of ^{241}Am, ^{154}Eu, ^{60}Co, ^{234}U, ^{235}U, ^{236}U, ^{239}Pu, ^{240}Pu and ^{241}Pu when they were missing or below the detection limits (Table S1). When not measured, the ^{232}Th concentration was considered equal to the mean of ^{232}Th concentrations in all soil samples.

Estimation of the total absorbed dose rate by prokaryotic cell

In the absence of any method to measure the total absorbed dose rates (TADR) by prokaryotic cell, TADR values were calculated based on soil RN activities. For this, two irradiation pathways were considered in the calculation: the external irradiation from the radio-contaminated habitat of bacteria and archaea (*i.e.* the soil) and the internal irradiation resulting from the internalization of RN in the cells (Garnier-Laplace *et al.* 2015).

The external and internal dose rates were calculated at each sampling point and for each sampling date by multiplying the Dose Conversion Coefficient (DCC) for each RN by the measured RN concentration at this sampling point or in the cells, respectively. The RN concentration inside the cells was considered in equilibrium with the soil RN concentration (conservatively assuming a concentration ratio of 1 for each RN) in the absence of any other

information. External and internal DCCs (Table S2A) were calculated for each RN with the EDEN software version 2.3 (Beaugelin-Seiller *et al.* 2006), assuming a different biological effectiveness for the different types of radiation (applied weighting factors were 10 for α-radiation, 3 for low β-radiation, and 1 for other β-radiation and γ-radiation) (Pröhl *et al.* 2003). The prokaryotic cells were described as a sphere with a 1-µm diameter, living in an infinitely extended and uniformly contaminated soil (compositions are provided in Table S2B).

Statistical analyses

Non-parametric tests (Kruskal-Wallis) were calculated using QIIME (Caporaso *et al.* 2010a). Redundancy Analysis was performed with R software (R Core Team 2011) on the OTUs and phylum abundance data with the Principal Component Analysis on Instrumental Variables (PCAIV) function of the ade4 package (Dray and Dufour, 2007). Heatmap was constructed with the gplots package of R (Bolker *et al* 2011).

Results

Overall prokaryotic diversity in the Chernobyl soils

This study focused on the prokaryotic communities in 36 soil samples collected inside and outside the RN-contaminated trench T22 at nine different positions in April and October 2009 (Figure 1). The pH values ranged from 4.4 to 6.1 and soil water content ranged from 2.2% to 7.3% (Table 1). The NaOH extractable organic C content ($C_{org(NaOH)}$) was within the same range for all samples (average 2.25±0.83g kg^{-1}), except for samples 4, 13, and 14 which were lower in content (average 0.35±0.30 g kg^{-1}). Soils collected within the trench (sample numbers 1, 3, 4, 8, 10 and 12) were contaminated with RNs (^{137}Cs activity ranging from 61 – 750 Bq g^{-1}), whereas soils collected in the vicinity of trench T22 (sample numbers 13, 14 and

20) exhibited low RN levels (^{137}Cs ranging from 0.35 – 1.50 Bq g^{-1}; Table 1). Three soil subsamples from October 2009 (designated as a, b and c) were used for DNA extraction in order to assess the reproducibility of the experiment. After quality filtering, we obtained 753 703 reads with a read length average of 255 bp, ranging from 16 182 – 23 686 reads in the 36 samples (Table 1). From the reads, 8 167 OTUs at 3% genetic distance were identified and after normalization of the dataset to 16 182 reads per sample and deletion of singletons, 7 663 OTUs were identified with OTU counts varying between 633 – 2 120 per sample (Table 1). The rarefaction curves based on PD whole tree, Chao1 and Shannon estimators tended to reach an asymptote (Figure S2). The Good's estimator of coverage varied between 95 – 98% across the samples, indicating that the depth of sequencing was nearly sufficient to detect most of the dominant OTUs (Table 1).

Of the reads, 95.7% were affiliated with Bacteria and 4.3% were affiliated with Archaea. The most consistently detected bacterial phyla (relative abundance > 1%) across all samples were *Proteobacteria*, *Acidobacteria*, AD3, *Planctomycetes*, *Chloroflexi*, *Verrucomicrobia* and *Actinobacteria*, with an uneven distribution across the samples (Figure 1). Combined, these seven groups accounted for 83.3% of the sequences. Twenty-seven additional bacterial phyla were detected as well as three archaeal phyla.

Trench T22 hosts specific microbiota

The rarefaction curves calculated using different estimators revealed a higher apparent species richness in almost all samples collected in the trench, as compared to the samples collected outside of the trench (Table 1). Accordingly, mean Chao1 richness and Shannon diversity indices were significantly higher in samples collected inside as opposed to outside the trench ($p < 0.05$; Figure S2).

Principal Coordinates Analysis (PCoA) based on bacterial and archaeal OTUs and performed with Bray-Curtis, Unweighted and Weighted Unifrac methods all showed a clear separation between the communities inside and outside the trench (Figure 2). The first principal components of the PCoA accounted for 20 – 40% of the variation between the samples, depending on the method used. Some divergence between samples taken at the same location in April and in October could be observed, particularly for samples collected within the trench. By contrast, high consistency between replicates (labeled as 'a', 'b' or 'c') was observed for each soil sample collected in October 2009, indicating high reproducibility of the experimental procedure.

Impact of long-term exposure to radioactive contaminated wastes on prokaryotic microbiota

To examine how the prokaryotic microbiota was affected by radioactivity, the TADR was calculated for each soil sample. On average, estimated TADR by cell were two orders of magnitude higher in trench soils than in samples collected outside of the trench; the maximum TADR was *ca.* 150 mGy h^{-1} in sample 8 in October 2009, whereas the lowest value was 0.1 mGy h^{-1} in samples 13 and 20 in April and October 2009, respectively (Table 1). Internal absorbed dose rates contributed to only 3% of the estimated TADR by cell (Table S3A and B) which is mainly due to the small size of prokaryotic cells. Actinides were the primary contributors to the estimated TADR by cell, and ^{239}Pu and ^{240}Pu were responsible for 80 – 96% of the estimated TADR by cell (Table S3A and B). Since the PCoA analysis was able to confirm the reproducibility of the experiment, the triplicates performed in October were averaged in order to create a single dataset and to facilitate depiction of the data. A redundancy analysis (RDA) coupled to a permutation test (randtest function) was used to test whether the community composition at the different sampling sites was related to the physico-chemical properties of the soil samples (Ramette 2007). The four physico-chemical variables

included in the analysis (TADR, $C_{org(NaOH)}$, water content, and pH) significantly explained 43% of the variation of the bacterial and archaeal communities ($r^2 = 0.43$, $p = 0.001$ based on 999 permutations). The first two axes of the RDA explain 85% of the variance due to the soil physico-chemical properties, 71% of which is accounted for by the first axis, which correlated primarily with TADR ($r = -0.90$), $C_{org(NaOH)}$ ($r = -0.84$) and water content ($r = -0.76$) (Figure 3). Using the RDA function in the 'vegan' package to separately analyze the effect of each variable indicates that TADR was the principal variable to influence the prokaryotic communities at the OTU-level ($p < 0.05$).

The same analysis at the phylum level confirmed the effect of the environmental variables on the bacterial communities since 52 % of the variation of the prokaryotic communities at the phylum level were explained by the environmental variables ($r^2 = 0.523$, $p = 0.001$ based on 999 permutations). The first two axes of the RDA explained 92 % of the variance, among which 74 % is explained by the first axis which correlated mainly with TADR ($r = -0.89$) and to a lesser extent with $C_{org(NaOH)}$ ($r = -0.69$) and water content ($r = -0.66$) (data not shown). The analysis of the effect of each variable separately showed that the principal variable influencing the prokaryotic communities at the phylum level were TADR ($p < 0.05$) and $C_{org(NaOH)}$ ($p < 0.1$).

Primary differences between prokaryotic microbiota of the trench and surrounding soils

Non-parametric tests (Kruskal-Wallis) were used to determine the significance of differences in prokaryotic diversity between samples and to identify the taxa representative of either the trench or the surrounding soils. This analysis revealed that among the 7 663 OTUs identified, 1 781 OTUs displayed significant changes in abundance between the highly contaminated trench soils and the low-contamination surrounding soils ($p < 0.05$). Specifically, 973 OTUs were significantly more abundant in the trench soils than in the

surrounding soils, whereas 808 OTUs were significantly more abundant in the surrounding soils than in the trench soils. Furthermore, these 1 781 OTUs accounted for 50% of the total prokaryotic microbiota in the trench and for 67% of the total prokaryotic microbiota in the surrounding soils, and could be classified into 26 bacterial phyla and three archaeal phyla.

To further explore the primary differences between microbiota of the trench soils and surrounding soils, a heatmap was constructed with the most abundant OTUs (> 1% relative abundance in at least one sample; see Table S4 for details) differing significantly between the trench and the surrounding soil microbiota (Figure 4). The surrounding soils were characterized by 20 abundant OTUs affiliated with the phyla *Crenarchaeota* (NRP-J order), *Acidobacteria* (Ellin6513, 32-20, DS-18 orders), *Actinobacteria* (*Mycobacterium* genus and MB-A2-108 class), AD3 (ABS-6 and JG37-AG-4 classes), *Gemmatimonadetes* (Gemm-1 class), *Verrucomicrobia* (DA101 genus) and WPS-2 (Figure 4). On the other hand, the trench prokaryotic community was characterized by 19 abundant OTUs. These OTUs were affiliated with the phyla *Crenarchaeota* (SAGMA-X family), *Acidobacteria* (11-24, Ellin6513, DS-18 orders), AD3 (ABS-6 and JG37-AG-4 classes), *Chloroflexi* (*Ktedonobacteraceae* family), *Proteobacteria* (*Bradyrhizobium*, *Rhodoplanes* and *Burkholderia* genera, SC-I-84 order and *Sinobacteraceae* family), *Verrucomicrobia* (auto67-4W family) and WPS-2 (Figure 4). Within the Archaea, the representative sequence of OTU 1143180 (*Crenarchaeota* (SAGMA-X)) exhibited 100% sequence similarity with *Candidatus* Nitrosotalea devanaterra, an acidophilic ammonia oxidizer (Lehtovirta-Morley *et al.* 2011), as well as sequences detected in acid water from a gold mine (AB050208; Takai *et al.* 2001). The OTUs specific to the trench did not have any cultured representatives within the Bacteria, with the exception of *Bradyrhyzobium*, *Rhodoplanes*, *Burkholderia* and *Sinobacteraceae*.

Relationships with other environments were investigated by performing a BLAST search of the non-redundant database, using representative sequences of the 19 OTUs specific

to the trench soils. Interestingly, among the closest neighbors (98 – 100% sequence similarity), we found sequences derived not only from a wide range of forest soils (data not shown) but also from cold environments (alpine tundra, boreal wetlands and forest, Finland, Himalayan mountains, Alaska, Iceland, Greenland, Antarctic habitats, the Arctic), acidic environments (acid water, acid mine drainage, acidic fen soil, acidic subalpine forest, acidic wetland), volcanic soils (Kasatochi Island in Alaska, a lava forest soil in Korea, Hawaiian volcanic deposit), RN- and heavy metal-contaminated soils, sediment and water samples (neptunium-contaminated sediments, soil samples of uranium mining waste pile, acid water from gold and potassium mines, lead-contaminated forest soil) as shown in Table S5. The representative sequence of OTU 573135, which is affiliated with *Bradyrhizobium*, was reported to have a 100% sequence similarity with many sequences, including a bacterium cultured from dust samples from the International Space Station (ISS) (LT617088; Mora *et al.* 2016).

Representation of cultured isolates in the prokaryotic community

We previously characterized a collection of 303 isolates recovered from Chernobyl soil samples by 16S rDNA partial sequencing (Chapon *et al.* 2012). Here, we analyzed whether the 284 isolates with available appropriate sequence data (*i.e.* the V4 domain of the 16S rDNA) were detected in the pyrosequencing dataset, and if they represent an abundant taxon in the prokaryotic community. In total, 206 sequences derived from isolates exhibited at least 97% sequence similarity with a pyrotag, falling within 47 OTUs of the pyrosequencing dataset. 183 isolates fall within 42 OTUs that represented a very minor fraction of the community across all samples, since altogether they accounted for less than 0.2% of the total. By contrast, 23 isolates fall within 5 well-represented OTUs (maximum relative abundance ranging from 0.71 – 6.97%): OTUs 125947, 156722, 196652, and 4057260, all affiliated to

Burkholderia spp. and OTU 573135, affiliated to *Bradyrhizobium* spp. (Table S6). The relative abundance of OTUs 4057260 and 573135 reached 6.97% and 2.90%, respectively, in the most contaminated soil (750 Bq/g of ^{137}Cs), which was collected in October 2009 at sampling point 3 (sample 3O; Tables 1 and S6). Furthermore, OTUs 125947 and 573135 are characteristic of the trench prokaryotic community.

Discussion

The current work explored the diversity of soil prokaryotes that have been evolving since more than two decades in RN-contaminated soils inside and outside of the trench T22, located within the Chernobyl exclusion zone. The presence of complex prokaryotic communities in contaminated soil and control samples from this site was revealed by a genetic fingerprint method (DGGE) in our previous study (Chapon *et al.* 2012). We observed that apparent diversity in the trench soils was similar to that observed in the surrounding soils on DGGE. However, this approach did not uncover any dominant community fingerprint clearly related to RN content, nor did it provide any direct taxonomic information. Here, we revisited this previous work to address these issues using 454 pyrosequencing of 16S rRNA genes. We surveyed the prokaryotic diversity of this understudied environment, and we assessed the effects of RN contamination and $C_{org(NaOH)}$ content on soil microbiota using a comparative analysis with low-contamination soils collected outside of the trench in the same area. The ^{137}Cs content in the soil samples collected outside of the trench is consistent with worldwide upper background levels of ^{137}Cs due to Chernobyl fallout (*e.g.* in France: from 0.01 - 0.1 Bq g^{-1} in upper soils, max value in hotspots: 10 Bq g^{-1}; IRSN, 2016). In addition, Michel *et al.* (2015) reported several values for Ukraine (from 0.3 mBq g^{-1} to 6.6 Bq g^{-1}) outside of the Chernobyl exclusion zone.

The seven dominant bacterial phyla in the Chernobyl soils were *Proteobacteria*, *Acidobacteria*, AD3, *Planctomycetes*, *Chloroflexi*, *Verrucomicrobia* and *Actinobacteria*. These phyla are commonly encountered as the dominant taxa in soils (Janssen 2006; Rastogi *et al.* 2009). Here, the abundance of *Chloroflexi* (mean relative abundance 9.4%, ranging from 2.4 – 16.1%) and AD3 (mean relative abundance 14.8%, ranging from 3.3 – 39.0%) was high, both inside and outside the trench. On a global scale, this is the most noticeable feature of Chernobyl soil prokaryotic communities. This high abundance is not an artefact linked to DNA extraction or PCR amplification, since other soil samples processed in the same experimental run did not exhibit the same profile (data not shown). High abundance of *Chloroflexi*/AD3 has been described in cold environments (Costello and Schmidt 2006; Taş *et al.* 2014; Hultman *et al.* 2015; Frey *et al.* 2016). Members of *Chloroflexi*/AD3 are reported to predominate following acute gamma irradiation of soils (McNamara *et al.* 2007; El-Sayed and Ghanem 2009) and have been detected in natural uranium ores (Mondani *et al.* 2011) and in uranium-contaminated sites (Selenska-Pobell 2002; Barns *et al.* 2007; Hug *et al.* 2013). It has been proposed that degradation of plant polymers is widespread across this phylum (Hug *et al.* 2013). Thus, members of this phylum are well-adapted to cold environments; they are potentially able to degrade lignocellulosic material; and they can tolerate uranium and/or its associated radioactivity. The high abundance of *Chloroflexi*/AD3 members both inside and outside trench T22 is coherent, taking into account the facts that Chernobyl upper soils are partly frozen during winter (Bixio *et al.* 2002), that wood debris were buried in the trench, and that bacteria and archaea are exposed to different levels of irradiation and contamination whether they are inside or outside of the trench. Nevertheless, when examining the results in greater detail, we noted that specific phylotypes within *Chloroflexi*/AD3 were selected by the soil trench. Indeed, the abundance of seven OTUs affiliated with classes ABS-6 and JG37-AG-4 was dramatically reduced in the trench, whereas three OTUs from the same classes

were strongly enriched in the trench, suggesting that these phylotypes may have distinct ecological niches and physiological characteristics such as tolerance to RNs exposure.

Our detailed comparative analysis of soils collected inside and outside the trench has revealed several specific patterns of soil prokaryotic assemblages. First, the Chao1 richness and Shannon diversity indices were significantly higher inside the trench as compared to the samples collected outside of the trench. On average, 1 589 observed OTUs were detected in the trench soils, whereas 1 103 OTUs were detected in the surrounding soils, indicating a positive effect of trench conditions on diversity. This had not been evidenced in our previous study, probably because of the limitation of DGGE to resolve complex profiles. Second, the PCoA ordination demonstrated significant differences between the prokaryotic communities from the trench and the surrounding area. When the trenches were dug, large amounts of highly irradiated and contaminated wood debris were buried, providing a considerable input of RNs as well as organic matter into this oligotrophic environment. The introduction of organic matter is expected to enhance diversity either by stimulating heterotrophic microorganisms which were already present as minor species, or by introducing new species from outside of the site. For instance, Field *et al.* (2010) showed that bacterial diversity was significantly enhanced upon cellulosic waste burial in the soil, with a corresponding shift in OTU number from approximately 750 to 1 600. By contrast, RN contamination is expected to have a negative impact on microbial communities due to radiotoxicity. According to Field *et al.* (2010), the impact of organic matter in the trench should have been larger than that actually observed in this study. We thus hypothesized that the presence of RNs counterbalanced the positive effect of lignocellulosic material on prokaryotic diversity in the trench, which would suggest that the RNs remaining in the trench still exert a negative impact on the prokaryotic communities. This hypothesis is supported by the statistical analysis of the data, since the RDA coupled to a permutation test revealed that the principal variable, among

all measured variables, influencing the prokaryotic communities at the OTU and phylum level was TADR and to a lesser extent $C_{org(NaOH)}$ when the analysis was performed at the phylum level. However, we could not exclude that other confounding factors not monitored during our study might also have influenced the prokaryotic communities composition.

808 OTUs were significantly enriched in the prokaryotic community outside of the trench, including 20 abundant OTUs. These abundant OTUs were affiliated to different phyla and do not have any cultured representatives, with the exception of *Mycobacterium*. Members of these phylotypes probably correspond to RN-sensitive species and/or oligotrophic microorganisms. We also identified specific OTUs that distinguished the trench microbiota from surrounding microbiota, indicating that specific phylotypes were selected by the trench soils. Close relationships with a wide range of cold environments and acidic soils were revealed, as well as volcanic soils or soils that have been subjected to fire, showing that traces of past events are still detectable in the trench prokaryotic community. In addition, relationships with radioactive environments were shown for five OTUs specific to the trench soils. Thus, members of the phylotypes that were selected by the trench conditions, in particular by high TADR, may have the capacity to survive under stressful conditions. These phylotypes are distributed among several phyla, illustrating that adaptation to life in radioactive environment is widespread in prokaryotes.

A limited number of reads from the 454 dataset identified as *Deinococcus* were detected in the soil samples, representing a very minor fraction of the total abundance (0.004 – 0.084%; mean relative abundance 0.017%). However, we failed to confirm the presence of this bacterium in Chernobyl soils using specific primers (Theodorakopoulos *et al.* 2013), suggesting that the very low relative abundance is the consequence of sequencing errors or PCR bias. Furthermore, *Deinococcus*-related species were not identified among the cultured bacteria retrieved from the soil samples (Chapon *et al.* 2012). Taken together, these results

strongly suggest that *Deinococcus* are either absent or are in extremely low abundance in this environment. This may be related to the high moisture content of Chernobyl soils, whereas *Deinococcus* members have been shown to be well-adapted to dry or low-moisture soils (Fredrickson *et al.* 2004; Chanal *et al.* 2006; Theodorakopoulos *et al.* 2013; Li *et al.* 2015).

Finally, the identification of representatives of two abundant OTUs typical of trench microbiota (OTU 125947 and 573135) in our culture collection has yielded some interesting results. These isolates, related to the genera *Bradyrhizobium* and *Burkholderia*, represent appropriate models for assessing the impact of long-term RN exposure on bacteria. Future studies could focus on these isolates to help determine the mechanisms of adaptation to this very unusual ecological niche.

Conclusion

In this study, we demonstrated that prokaryotic communities from Chernobyl disposal trench T22, as well as samples collected in the proximity, share common traits with prokaryotic assemblages from cold environments on a global scale although a significant difference in diversity and community composition could be observed between the trench and its proximal environment. Our results indicate that the introduction of contaminated lignocellulosic material within trench T22 has shaped prokaryotic communities by modifying species composition and abundance. In this regard, TADR was the principal variable to influence the prokaryotic communities while still exerting a negative effect on prokaryotic diversity. We identified specialized phylotypes that have successfully colonized the trench, two of which have cultured representatives in our culture collection. Further work, such as shotgun metagenome sequencing and experiments on these bacterial isolates, may be helpful in determining the function of bacterial communities in this ecosystem.

Funding

This work was supported by the National Center for Scientific Research and the Institute for Radioprotection and Nuclear Safety through the TRASSE GNR (Research Action Number 2009-1A). Nicolas Theodorakopoulos was the recipient of a PhD grant co-funded by the Institute for Radioprotection and Nuclear Safety and the Provence Alpes Côtes d'Azur regional council.

Acknowledgements

We thank Brandon Loveall of Improvence for English proofreading of the manuscript.

Conflict of interest: The authors declare no conflicts of interest.

References

Akob DM, Mills HJ, Kostka JE. Metabolically active microbial communities in uranium-contaminated subsurface sediments. *FEMS Microbiol Ecol* 2007;**59**:95-107.

Barns SM, Cain EC, Sommerville L *et al. Acidobacteria* phylum sequences in uranium-contaminated subsurface sediments greatly expand the known diversity within the phylum. *Appl Environ Microbiol* 2007;**73**:3113-6.

Beaugelin-Seiller K, Jasserand F, Garnier-Laplace J *et al.* Modelling the radiological dose in non-human species: principles, computerization and application. *Health Phys* 2006;**90**:485-493.

Bixio A, Gambolati G, Paniconi C *et al.* Modeling groundwater-surface water interactions including effects of morphogenetic depressions in the Chernobyl exclusion zone. *Environ Geol* 2002;**42**:162-77.

Bolker B, Bonebakker L, Gentleman R *et al.* gplots: Various R programming tools for plotting data. (2011). R package version 2.10.1.

Bugai D, Kashparov V, Dewiére L *et al.* Characterization of subsurface geometry and radioactivity distribution in the trench containing Chernobyl clean-up wastes. *Environ Geol* 2005;**47**:869-81.

Caporaso JG, Bittinger K, Bushman FD *et al*. PyNAST: a flexible tool for aligning sequences to a template alignment. *Bioinformatics* 2010a;**26**:266-67.

Caporaso JG, Kuczynski J, Stombaugh J *et al*. QIIME allows analysis of high-throughput community sequencing data. *Nat Methods* 2010b;**7**:335-6.

Chanal A, Chapon V, Benzerara K *et al.* The desert of Tataouine: an extreme environment that hosts a wide diversity of microorganisms and radiotolerant bacteria. *Environ Microbiol* 2006;**8**:514-25.

Chapon V, Piette L, Vesvres MH *et al.* Microbial diversity in contaminated soils along the T22 trench of the Chernobyl experimental platform. *Appl Geochem* 2012;**27**:1375-83.

Claesson MJ, O'Sullivan O, Wang Q *et al.* Comparative analysis of pyrosequencing and a phylogenetic microarray for exploring microbial community structures in the human distal intestine. *PLoS ONE* 2009;**4**:e6669.

Costello EK, Schmidt SK. Microbial diversity in alpine tundra wet meadow soil: novel *Chloroflexi* from a cold, water-saturated environment. *Environ Microbiol* 2006;**8**:1471-86.

Czirják GA, Møller AP, Mousseau TA *et al.* Microorganisms associated with feathers of barn swallows in radioactively contaminated areas around Chernobyl. *Microbiol Ecol* 2010;**60**:373-80.

DeSantis TZ, Hugenholtz P, Larsen N et al. Greengenes, a chimera-checked 16S rRNA gene database and workbench compatible with ARB. *Appl Environ Microb* 2006;**72**:5069-72.

Dowd SE, Callaway TR, Wolcott RD *et al.* Evaluation of the bacterial diversity in the feces of cattle using 16S rDNA bacterial tag-encoded FLX amplicon pyrosequencing (bTEFAP). *BMC Microbiol* 2008;**8**:125.

Dray S, Dufour AB. The ade4 package: implementing the duality diagram for ecologists. *J Stat Software* 2007;**22**:1-20.

Edgar RC. Search and clustering orders of magnitude faster than BLAST. *Bioinformatics* 2010;**26**:2460-61.

El-Sayed WS, Ghanem S. Bacterial Community Structure Change Induced by Gamma Irradiation in Hydrocarbon Contaminated and Uncontaminated Soils Revealed by PCR-Denaturing Gradient Gel Electrophoresis. *Biotechnol* 2009;**8**:78-85.

Field EK, D'Imperio S, Miller AR *et al.* Application of molecular techniques to elucidate the influence of cellulosic waste on the bacterial community structure at a simulated low-level-radioactive-waste site. *Appl Environ Microbiol* 2010;**76**:3106-15.

Fields MW, Yan T, Rhee SK *et al.* Impacts on microbial communities and cultivable isolates from groundwater contaminated with high levels of nitric acid-uranium waste. *FEMS Microbiol Ecol* 2005;**53**:417-28.

Fredrickson JK, Zachara JM, Balkwill DL *et al.* Geomicrobiology of high-level nuclear waste-contaminated vadose sediments at the Hanford Site, Washington State. *Appl Environ Microbiol* 2004;**70**:4230-241.

Frey B, Rime T, Phillips M *et al.* Microbial diversity in European alpine permafrost and active layers. *FEMS Microbiol Ecol* 2016;92(3).

Garnier-Laplace J., Beaugelin-Seiller K *et al.* Radiological dose reconstruction for birds reconciles outcomes of Fukushima with knowledge of dose-effect relationships. *Scientific Reports* 2015;**5**:16594.

Geissler A, Selenska-Pobell S. Addition of U(VI) to a uranium mining waste sample and resulting changes in the indigenous bacterial community. *Geobiology* 2005;**3**:275-85.

Hu QH, Weng JQ, Wang JS. Sources of anthropogenic radionuclides in the environment: a review. *J Environ Radioact* 2008;**101**:426-37.

Hug LA, Castelle CJ, Wrighton KC *et al.* Community genomic analyses constrain the distribution of metabolic traits across the *Chloroflexi* phylum and indicate roles in sediment carbon cycling. *Microbiome* 2013;1:22.

Hultman J, Waldrop MP, Mackelprang R *et al.* Multi-omics of permafrost, active layer and thermokarst bog soil microbiomes. *Nature* 2015;**521**:208-12.

IRSN. Constat Radiologique "Rémanence de la radioactivité d'origine artificielle" ». Rapport de mission 2016. http://www.irsn.fr/FR/expertise/rapports_expertise/surveillance-environnement/Documents/IRSN_Constat-Remanence-France_201604.pdf

Islam E, Sar P. Culture-dependent and -independent molecular analysis of the bacterial community within uranium ore. J Basic Microbiol 2011;**51**:372-84.

Islam E, Paul D, Sar P. Microbial Diversity in Uranium Deposits from Jaduguda and Bagjata Uranium Mines, India as Revealed by Clone Library and Denaturing Gradient Gel Electrophoresis Analyses. *Geomicrobiol J* 2014;**31**:862-874.

Janssen PH. Identifying the dominant soil bacterial taxa in libraries of 16S rRNA and 16S rRNA genes. *Appl Environ Microbiol* 2006;**72**:1719-728.

Kashparov VA, Lundin SM, Khomutinin YV *et al.* Soil contamination with ^{90}Sr in the near zone of the Chernobyl accident. *J Environ Radioact* 2001;**56**:285-98.

Klindworth A, Pruesse E, Schweer T *et al.* Evaluation of general 16S ribosomal RNA gene PCR primers for classical and next-generation sequencing-based diversity studies. 2013 Nucleic Acids Res 2013;**41**(1):e1.

Kumar, R., Nongkhlaw, M., Acharya, C., Joshi, S. R. Bacterial community structure from the perspective of the uranium ore deposits of Domiasiat in India. *Proc Nat Acad Sci, India Section B: Biological Sciences* 2013;**83**:485-97.

Lehtovirta-Morley LE, Stoecker K, Vilcinskas A *et al.* Cultivation of an obligate acidophilic ammonia oxidizer from a nitrifying acid soil. *Proc Natl Acad Sci U S A*. 2011;**108**:15892-7.

Li CH, Tang LS, Jia ZJ et al. Profile Changes in the Soil Microbial Community When Desert Becomes Oasis. *PLoS One* 2015;**10**(10):e0139626.

Lloyd JR, Macaskie LE. Chapter 11: Biochemical basis of microbe-radionuclide interactions, In: Keith-Roach, M.J., Livens, F.R. (Eds.) *Radioactivity in the Environment*. Netherlands:Elsevier Science 2002;313-42.

Lozupone C, Knight R. UniFrac: a new phylogenetic method for comparing microbial communities. *Appl Environ Microbiol* 2005;**71**:8228-35.

Martin-Garin A, Van Meir N, Simonucci C *et al.* Quantitative assessment of radionuclide migration from near-surface radioactive waste burial sites: the waste dumps in the Chernobyl exclusion zone as an example. In: Poinssot C, Geckeis H (ed.). Radionuclide behaviour in the natural environment. Science, implications and lessons for the nuclear industry. Woodhead Publishing Series in Energy: Number 42, 2012, 570-600.

Mora M, Perras A, Alekhova TA *et al.* Resilient microorganisms in dust samples of the International Space Station-survival of the adaptation specialists. *Microbiome* 2016;**4**:65.

McNamara NP, Griffiths RI, Tabouret A. *et al.* The sensitivity of a forest soil microbial community to acute gamma-irradiation. *Appl Soil Ecol* 2007;**37**:1-9.

Merroun M, Selenska-Pobell S. Bacterial interactions with uranium: an environmental perspective *J Cont Hydrol* 2008;**102**:285-95.

Michel R, Daraoui A, Gorny M *et al.* A retrospective dosimetry of Iodine-131 exposure using Iodine-129 and Caesium-137 inventories in soils – A critical evaluation of the consequences of the Chernobyl accident in parts of Northern Ukraine. *J Environ Radioact* 2015;**150**:20-35.

Mondani L, Benzerara K, Carrière M *et al.* Influence of Uranium on Bacterial Communities: A Comparison of Natural Uranium-Rich Soils with Controls. *PLoS ONE* 2011;**6**:e25771.

Newsome L, Morris K, Lloyd JR. The biogeochemistry and bioremediation of uranium and other priority radionuclides. *Chem Geol* 2014;**363**:164-84.

Niedrée B, Berns AE, Vereecken H *et al.* Do Chernobyl-like contaminations with (137)Cs and (90)Sr affect the microbial community, the fungal biomass and the composition of soil organic matter in soil? *J Environ Radioact* 2013;**118**:21-9.

Pröhl G, Brown J, Gomez-Ros J-M *et al.* Dosimetric models and data for assessing radiation exposures to biota. 2003. Deliverable3, FASSET project, Contract n° FIGE-CT- 2000-00102.

Radeva, G., Kenarova, A., Bachvarova, V. *et al*. Bacterial diversity at abandoned uranium mining and milling sites in Bulgaria as revealed by 16S rRNA genetic diversity study. *Water Air Soil Pollut* 2013;**224**:1748.

Ragon M, Restoux G, Moreira D. *et al.* Sunlight-exposed biofilm microbial communities are naturally resistant to Chernobyl ionizing-radiation levels. *PLoS One* 2011;**6**:e21764.

Ramette A. Multivariate analyses in microbial ecology. *FEMS Microbiol Ecol* 2007;**62**:142-160.

Rastogi G, Stetler L, Peyton B *et al.* Molecular analysis of prokaryotic diversity in the deep subsurface of the former Homestake gold mine, South Dakota, USA. *J Microbiol* 2009;**47**:371-84.

Rastogi G, Osman S, Vaishampayan PA *et al.* Microbial diversity in uranium mining-impacted soils as revealed by high-density 16S microarray and clone library. *Microb Ecol* 2010;**59**:94-108.

R Core Team. R: A Language and Environment for Statistical Computing. R Foundation for Statistical Computing, Vienna, Austria (http://www.R-project.org). 2011

Romanovskaya VA, Sokolov IG, Rokitko PV *et al.* Ecological consequences of radioactive pollution for soil bacteria within the 10-km region around the Chernobyl Atomic Energy Station. *Mikrobiologiia* 1998;**67**:274–80.

Romanovskaya VA, Rokitko PV, Malashenko YR *et al.* Sensitivity of soil bacteria isolated from the alienated zone around the Chernobyl nuclear power plant to various stress factors. *Mikrobiologiia* 1999;**68**:465-69.

Romanovskaya VA, Rokitko PV, Malashenko YR. Unique properties of highly radioresistant bacteria. *Mikrobiologiia* 2000;**62**:40–63.

Selenska-Pobell S, Kampf G, Hemming K, Radeva G, Satchanska G. Bacterial diversity in soil samples from two uranium waste piles as determined by rep-APD, RISA and 16S rDNA retrieval. *Antonie Van Leeuwenhoek* 2001;**79**:149-61.

Selenska-Pobell S. Chapter 8: Diversity and activity of bacteria in uranium waste piles, In: Keith-Roach, M.J., Livens, F.R. (Eds.) Radioactivity in the Environment. Netherlands:Elsevier Science, 2002;225-254.

Takai K, Moser DP, DeFlaun M *et al*. Archaeal diversity in waters from deep South African gold mines. *Appl Environ Microbiol*. 2001;**67**:5750-60.

Taş N, Prestat E, McFarland JW *et al.* Impact of fire on active layer and permafrost microbial communities and metagenomes in an upland Alaskan boreal forest. *ISME J* 2014;**8**:1904-19.

Theodorakopoulos N, Bachar D, Christen R *et al.* Exploration of *Deinococcus-Thermus* molecular diversity by novel group-specific PCR primers. *MicrobiologyOpen* 2013;**2**:862-72.

Theodorakopoulos N, Chapon V, Coppin F *et al.* Use of combined microscopic and spectroscopic techniques to reveal interactions between uranium and Microbacterium sp. A9, a strain isolated from the Chernobyl exclusion zone. *J Hazard Mater* 2015;**285**:285-93.

Vazquez-Baeza Y, Pirrung M, Gonzalez A *et al*. Emperor: A tool for visualizing high-throughput microbial community data. *Gigascience* 2013;**2**:16.

Waldron PJ, Wu L, Van Nostrand JD *et al.* Functional gene array-based analysis of microbial community structure in groundwaters with a gradient of contaminant levels. *Environ Sci Technol* 2009;**43**:3529-34.

Wang Q, Garrity GM, Tiedje JM *et al*. Naive Bayesian classifier for rapid assignment of rRNA sequences into the new bacterial taxonomy. *Appl Environ Microb* 2007 ;73: 5261-67.

Yan X, Luo X, Zhao M. Metagenomic analysis of microbial community in uranium-contaminated soil. *Appl Microbiol Biotechnol* 2016;**100**:299-310.

Yergeau E, Newsham KK, Pearce DA *et al.* Patterns of bacterial diversity across a range of Antarctic terrestrial habitats. *Environ Microbiol* 2007;**9**:2670-82.

Zavilgelsky GB, Abilev SK, Sukhodolets VV *et al.* Isolation and analysis of UV and radio-resistant bacteria from Chernobyl. *J Photochem Photobiol* 1998;**43**:152–7.

Soil sample	Sampling location	^{137}Cs (Bq g^{-1})	pH	$C_{org(NaOH)}$ (g kg^{-1})	Water content (%)	TADR (mGy h^{-1})	Subsample	number of high-quality reads	Observed OTUs	Chao1	Shannon diversity index	Good's estimator of coverage
1_A	inside	420	5.1	2.56	5.8	83		21 279	1 806	2 702	8.6	0.96
1_O	inside	420	4.8	2.61	7.3	86	a,b,c	19 818±1 094	2 087±42	3 030±78	9.3±0.1	0.95±0.00
3_A	inside	300	5.6	1.48	5.7	28		18 822	1 628	2 568	8.4	0.96
3_O	inside	750	5	1.77	5.1	153	a,b,c	20 827±1 469	1 622±36	2 433±29	8.0±0.2	0.96±0.00
4_A	inside	61	5.4	0.49	3.5	9		23 083	1 454	2 197	8.3	0.96
4_O	inside	140	4.8	0.88	5.1	29	a,b,c	20 931±489	1 478±47	2 324±51	8.4±0.2	0.96±0.00
8_A	inside	640	5.2	4.12	6.2	137		22 159	1 353	2 102	8.1	0.97
8_O	inside	670	4.5	2.93	3.6	137	a,b,c	23 603±90	1 498±24	2 278±54	8.4±0.1	0.96±0.00
10_A	inside	290	4.7	2.15	4.9	90		23 613	1 333	2 054	7.9	0.97
10_O	inside	710	4.9	2.77	5.2	145	a,b,c	21 544±2 042	1 524±27	2 275±11	8.5±0.1	0.96±0.00
12_A	inside	260	5.4	1.16	3.7	47		19 690	1 585	2 300	8.7	0.96
12_O	inside	370	4.4	1.48	4.8	76	a,b,c	21 515±1 521	1 452±4	2 277±82	8.3±0.0	0.96±0.00
13_A	outside	0.37	6.1	0.16	2.2	0.1		22 966	1 145	1 755	6.9	0.97
13o	outside	1.5	4.3	0.12	2.7	0.3	a,b,c	17 761±1 626	639±10	977±60	5.8±0.1	0.98±0.00
14_A	outside	0.91	6.1	0.1	2.5	0.4		22 291	969	1 355	7.2	0.98
14_O	outside	0.79	4.8	0.34	4.1	0.2	a,b,c	20 118±1 308	1 167±16	1 684±36	7.8±0.1	0.97±0.00
20_A	outside	0.35	5.4	1.99	4.7	0.3		23 354	1 424	2 108	8.2	0.97
20_O	outside	0.54	4.5	1.96	5.1	0.1	a,b,c	19 364±1 469	1 427±55	2 160±144	8.0±0.1	0.97±0.01

Table 1: Primary soil characteristics of samples collected inside and outside of trench T22. The table comprises soil physico-chemical parameters (from Chapon *et al*. 2012), total absorbed dose rates (TADR) by cell, OTU counts and estimators of alpha-diversity. In the soil sample name, "A" stands for April and "O" for October.

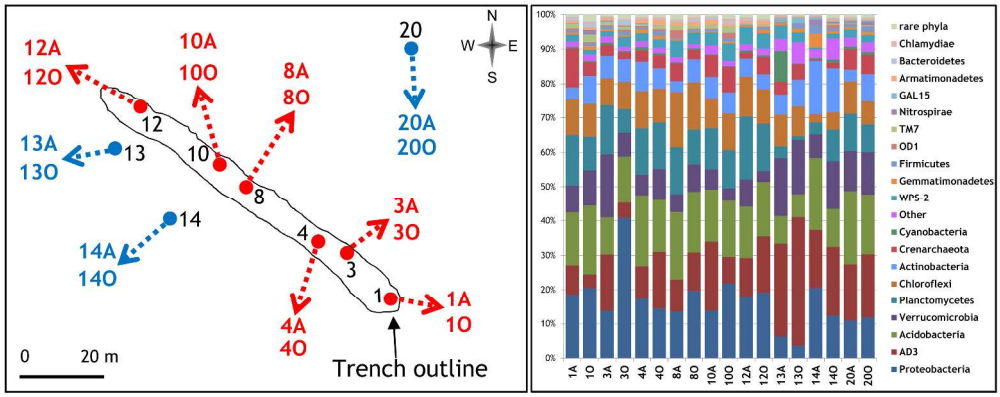

Figure 1: Location of the sampling points (left) and taxonomic profiles of the microbial communities (right), for soil samples collected in April (-A) and October (-O) 2009. The triplicate samples performed in October were combined.

1363x539mm (72 x 72 DPI)

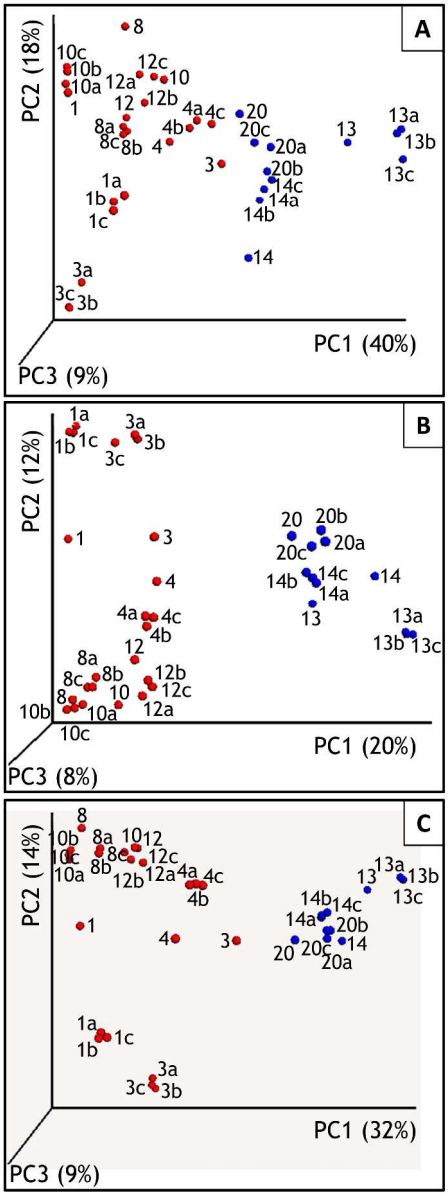

Figure 2: 3D Principal Coordinates Analysis (PCoA) plots of weighted UniFrac (A), unweighted UniFrac (B), and Bray−Curtis (C) distances between the soil samples collected in the trench (red) and in the surrounding soils (blue). Samples are identified with a number corresponding to the sampling position. To enhance readability, the samples collected in April 2009 are labelled with a single number, whereas the triplicates performed in October 2009 are labelled as Xa, Xb or Xc. The percent variation explained by the PCs is indicated on the respective axes and refers to the fraction of the total variance.

787x2091mm (72 x 72 DPI)

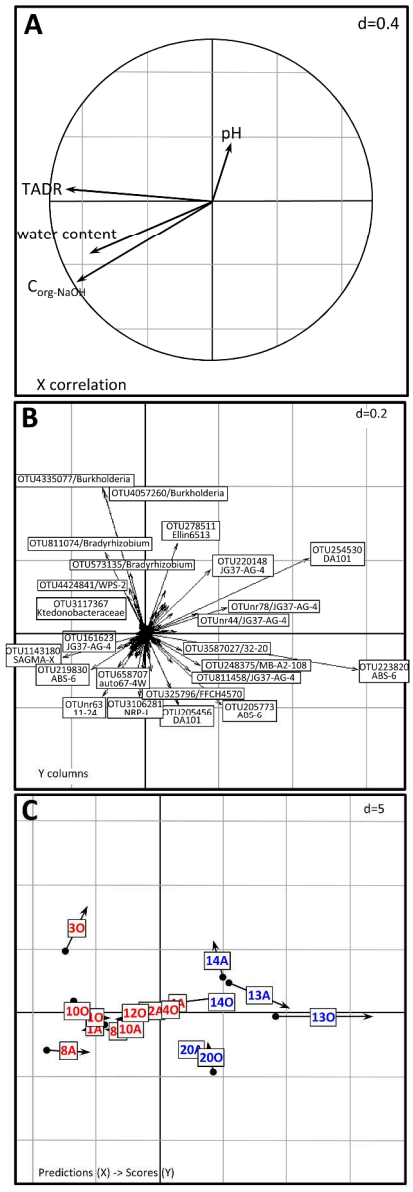

Figure 3: Multivariate redundancy analysis diagrams illustrating the relationship between the OTU-level community structure from soil samples collected in April (labelled with A) and October (labelled with O) 2009 and environmental parameters (TADR, Corg(NaOH), pH, and water content). A) correlation of physico-chemical explanatory variables with the first two axes of the PCAIV.; B) OTU scores. Only OTUs with the highest loadings are labelled with their ID number and lowest taxonomic rank. C) joint display of the position of the sampling sites by averaging (points) and by regression (arrowheads). Red: samples from the trench; blue: samples from the surrounding area.

694x2040mm (72 x 72 DPI)

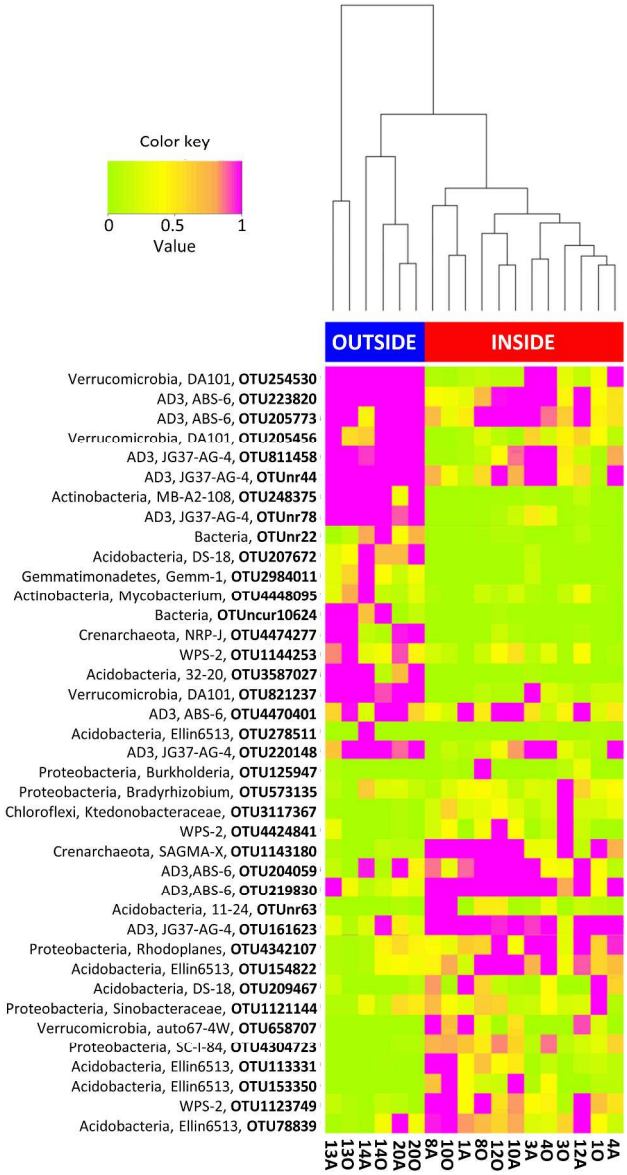

Figure 4: Cluster analysis of the soil samples and the corresponding heat map constructed with abundant OTUs (>1% relative abundance in at least one soil sample) differing significantly between the trench and the surrounding soil microbiota. Red: samples from the trench; blue: samples from the surrounding area. The highest and lowest taxonomic affiliations are indicated for each OTU.

808x1519mm (72 x 72 DPI)

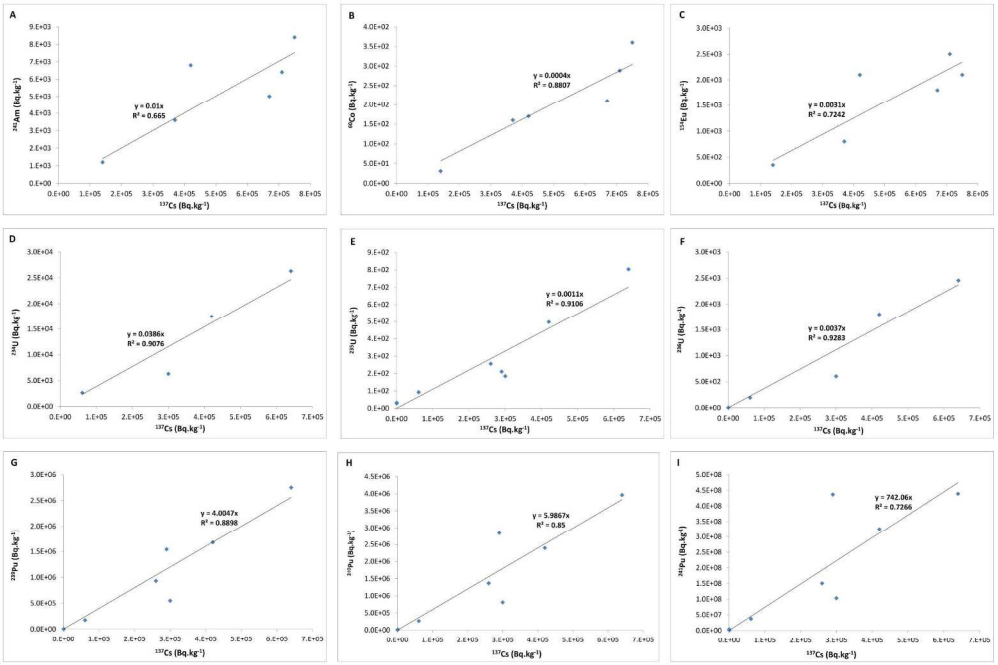

Figure S1: Relationship between measured concentrations (Bq.kg^{-1}) of ^{137}Cs and A) ^{241}Am, B) ^{61}Co, C) ^{154}Eu, D) ^{234}U, E) ^{235}U, F) ^{236}U, G) ^{239}Pu, H) ^{240}Pu and I) ^{241}Pu, at different soil sampling sites.

2116x1587mm (72 x 72 DPI)

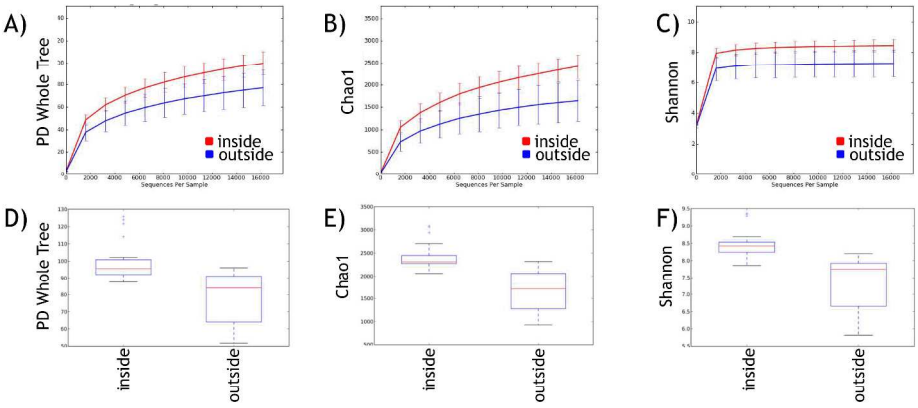

Figure S2 : Alpha rarefaction plots for Phylogenetic Distance Whole Tree (A), Chao1 (B) and Shannon (C) indices computed with the soil samples collected inside the trench (red) and outside (blue). The corresponding distance boxplots are shown in D), E) and F) respectively. The error bars show the standard error of the mean diversity.

2116x1587mm (72 x 72 DPI)

Table S1: Radionuclide concentrations (Bq.kg^{-1}) at the different soil sampling sites.

Soil sample	Soil radionuclide concentration (Bq.kg^{-1})[1]											
	^{137}Cs		^{90}Sr		^{241}Am		^{60}Co		^{154}Eu		^{234}U	
	Apr 09	Oct 09	Apr 09	Oct 09	Apr 09	Oct 09	Apr 09	Oct 09	Apr 09	Oct 09	Apr 09	Oct 09
1	4.20E+05	4.20E+05	2.25E+05	2.25E+05	*4.21E+03*	6.80E+03	*1.70E+02*	1.70E+02	*1.31E+03*	2.10E+03	1.75E+04	*1.62E+04*
3	3.00E+05	7.50E+05	1.60E+05	4.01E+05	*3.01E+03*	8.40E+03	*1.22E+02*	3.60E+02	*9.39E+02*	2.10E+03	6.28E+03	*2.89E+04*
4	6.10E+04	1.40E+05	3.26E+04	7.49E+04	*6.12E+02*	1.20E+03	*2.48E+01*	3.10E+01	*1.91E+02*	3.50E+02	2.65E+03	*5.40E+03*
8	6.40E+05	6.70E+05	3.42E+05	3.58E+05	*6.42E+03*	5.00E+03	*2.60E+02*	2.10E+02	*2.00E+03*	1.80E+03	2.63E+04	*2.58E+04*
10	2.90E+05	7.10E+05	1.55E+05	3.80E+05	*2.91E+03*	6.40E+03	*1.18E+02*	2.88E+02	*9.07E+02*	2.50E+03	*1.12E+04*	*2.74E+04*
12	2.60E+05	3.70E+05	1.39E+05	1.98E+05	*2.61E+03*	3.60E+03	*1.06E+02*	1.60E+02	*8.13E+02*	8.00E+02	*1.00E+04*	*1.43E+04*
13	3.70E+02	1.50E+03	1.98E+02	8.02E+02	*3.71E+00*	*1.51E+01*	*1.50E-01*	*6.09E-01*	*1.16E+00*	*4.69E+00*	*1.43E+01*	*5.78E+01*
14	9.10E+02	7.90E+02	4.87E+02	4.22E+02	*9.13E+00*	*7.93E+00*	*3.69E-01*	*3.21E-01*	*2.85E+00*	*2.47E+00*	*3.51E+01*	*3.05E+01*
20	3.50E+02	5.40E+02	1.87E+02	2.89E+02	*3.51E+00*	*5.42E+00*	*1.42E-01*	*2.19E-01*	*1.10E+00*	*1.69E+00*	*1.35E+01*	*2.08E+01*

Soil sample	Soil radionuclide concentration (Bq.kg^{-1})[1]											
	^{235}U		^{236}U		^{232}Th		^{239}Pu		^{240}Pu		^{241}Pu	
	Apr 09	Oct 09	Apr 09	Oct 09	Apr 09	Oct 09	Apr 09	Oct 09	Apr 09	Oct 09	Apr 09	Oct 09
1	4.96E+02	*4.60E+02*	1.80E+03	*1.56E+03*	1.54E+03	*1.55E+03*	1.68E+06	*1.68E+06*	2.39E+06	*2.51E+06*	3.26E+08	*3.12E+08*
3	1.84E+02	*8.22E+02*	6.02E+02	*2.78E+03*	1.75E+03	*1.55E+03*	5.49E+05	*3.00E+06*	8.09E+05	*4.49E+06*	1.03E+08	*5.57E+08*
4	9.25E+01	*1.53E+02*	1.92E+02	*5.19E+02*	1.44E+03	*1.55E+03*	1.73E+05	*5.61E+05*	2.66E+05	*8.38E+05*	3.72E+07	*1.04E+08*
8	8.04E+02	*7.34E+02*	2.45E+03	*2.48E+03*	1.65E+03	*1.55E+03*	2.75E+06	*2.68E+06*	3.96E+06	*4.01E+06*	4.39E+08	*4.97E+08*
10	2.10E+02	*7.78E+02*	*1.07E+03*	*2.63E+03*	1.69E+03	*1.55E+03*	1.54E+06	*2.84E+06*	2.84E+06	*4.25E+06*	4.37E+08	*5.27E+08*
12	2.55E+02	*4.05E+02*	*9.64E+02*	*1.37E+03*	1.46E+03	*1.55E+03*	9.30E+05	*1.48E+06*	1.37E+06	*2.22E+06*	1.50E+08	*2.75E+08*
13	2.84E+01	*1.64E+00*	*1.37E+00*	*5.56E+00*	1.43E+03	*1.55E+03*	*1.48E+03*	*6.01E+03*	*2.22E+03*	*8.98E+03*	*2.75E+05*	*1.11E+06*
14	2.98E+01	*8.66E-01*	*3.37E+00*	*2.93E+00*	1.25E+03	*1.55E+03*	3.38E+03	*3.16E+03*	1.47E+04	*4.73E+03*	1.34E+06	*5.86E+05*
20	3.20E+01	*5.92E-01*	2.18E+00	*2.00E+00*	1.78E+03	*1.55E+03*	*1.40E+03*	*2.16E+03*	8.58E+03	*3.23E+03*	3.91E+06	*4.01E+05*

[1] Values in italics were derived from the ^{137}Cs content.

Table S2: Parameters used for Total Dose Rate calculation with EDEN.

A: Internal and external Dose Conversion Coefficients (DCC) (µGy h^{-1} per Bq kg^{-1}) for prokaryotic cell.

DCC	^{137}Cs+	^{241}Am	^{60}Co	^{154}Eu	^{90}Sr+	^{234}U	^{235}U+	^{236}U	^{232}Th	239Pu	^{240}Pu	^{241}Pu
Internal	4.92E-06	1.98E-04	8.33E-06	8.08E-06	5.75E-07	1.95E-04	2.71E-04	2.03E-04	2.20E-04	1.87E-04	1.85E-04	6.58E-06
external	4.03E-05	2.00E-02	7.29E-05	5.67E-05	5.89E-05	1.78E-02	1.56E-02	1.60E-02	1.37E-02	1.96E-02	1.96E-02	4.54E-07

B: Soil and bacteria composition (% of total mass).

Element	**C**	**H**	**O**	**N**	**P**	**S**	**Ca**	**Na**	**K**	**Mg**	**Al**	**Si**	**Fe**
Bacteria	53.1	6.2	28.3	12.4									
Soil	0.18	0.9602	50.73	0.03001	0.11	0.11	3.261	2.39	2.31	2.11	7.401	26.17	4.241

Table S3: A) Internal absorbed dose rate (µGy.h^{-1})

Soil sample	Internal absorbed dose rate (µGy.h^{-1})											
	^{137}Cs		^{90}Sr		^{241}Am		^{60}Co		^{154}Eu		^{234}U	
	Apr 09	Oct 09	Apr 09	Oct 09	Apr 09	Oct 09	Apr 09	Oct 09	Apr 09	Oct 09	Apr 09	Oct 09
1	2.06E+00	2.06E+00	1.29E-01	1.29E-01	8.36E-01	1.35E+00	1.42E-03	1.42E-03	1.06E-02	1.70E-02	3.41E+00	3.16E+00
3	1.47E+00	3.69E+00	9.22E-02	2.31E-01	5.97E-01	1.67E+00	1.01E-03	3.00E-03	7.59E-03	1.70E-02	1.23E+00	5.65E+00
4	3.00E-01	6.88E-01	1.88E-02	4.30E-02	1.21E-01	2.38E-01	2.06E-04	2.58E-04	1.54E-03	2.83E-03	5.17E-01	1.05E+00
8	3.15E+00	3.29E+00	1.97E-01	2.06E-01	1.27E+00	9.92E-01	2.16E-03	1.75E-03	1.62E-02	1.46E-02	5.14E+00	5.05E+00
10	1.43E+00	3.49E+00	8.92E-02	2.18E-01	5.77E-01	1.27E+00	9.81E-04	2.40E-03	7.33E-03	2.02E-02	2.19E+00	5.35E+00
12	1.28E+00	1.82E+00	7.99E-02	1.14E-01	5.18E-01	7.14E-01	8.79E-04	1.33E-03	6.58E-03	6.47E-03	1.96E+00	2.79E+00
13	1.82E-03	7.37E-03	1.14E-04	4.61E-04	7.36E-04	2.99E-03	1.25E-06	5.07E-06	9.36E-06	3.79E-05	2.79E-03	1.13E-02
14	4.47E-03	3.88E-03	2.80E-04	2.43E-04	1.81E-03	1.57E-03	3.08E-06	2.67E-06	2.30E-05	2.00E-05	6.86E-03	5.95E-03
20	1.72E-03	2.65E-03	1.08E-04	1.66E-04	6.97E-04	1.07E-03	1.18E-06	1.83E-06	8.85E-06	1.37E-05	2.64E-03	4.07E-03

Soil sample	Internal absorbed dose rate (µGy.h^{-1})											
	^{235}U		^{236}U		^{232}Th		^{239}Pu		^{240}Pu		^{241}Pu	
	Apr 09	Oct 09	Apr 09	Oct 09	Apr 09	Oct 09	Apr 09	Oct 09	Apr 09	Oct 09	Apr 09	Oct 09
1	1.34E-01	1.25E-01	3.66E-01	3.16E-01	3.39E-01	3.42E-01	3.14E+02	3.15E+02	4.43E+02	4.65E+02	2.14E+03	2.05E+03
3	4.99E-02	2.23E-01	1.22E-01	5.65E-01	3.84E-01	3.42E-01	1.03E+02	5.62E+02	1.50E+02	8.31E+02	6.80E+02	3.66E+03
4	2.51E-02	4.15E-02	3.91E-02	1.05E-01	3.16E-01	3.42E-01	3.24E+01	1.05E+02	4.93E+01	1.55E+02	2.45E+02	6.84E+02
8	2.18E-01	1.99E-01	4.99E-01	5.05E-01	3.62E-01	3.42E-01	5.15E+02	5.02E+02	7.33E+02	7.42E+02	2.89E+03	3.27E+03
10	5.69E-02	2.11E-01	2.19E-01	5.35E-01	3.71E-01	3.42E-01	2.88E+02	5.32E+02	5.25E+02	7.86E+02	2.88E+03	3.47E+03
12	6.91E-02	1.10E-01	1.96E-01	2.79E-01	3.21E-01	3.42E-01	1.74E+02	2.77E+02	2.53E+02	4.10E+02	9.90E+02	1.81E+03
13	7.70E-03	4.45E-04	2.79E-04	1.13E-03	3.15E-01	3.42E-01	2.77E-01	1.12E+00	4.10E-01	1.66E+00	1.81E+00	7.33E+00
14	8.08E-03	2.34E-04	6.86E-04	5.95E-04	2.75E-01	3.42E-01	6.32E-01	5.92E-01	2.72E+00	8.75E-01	8.80E+00	3.86E+00
20	8.66E-03	1.60E-04	4.43E-04	4.07E-04	3.91E-01	3.42E-01	2.62E-01	4.05E-01	1.59E+00	5.98E-01	2.58E+01	2.64E+00

Table S3: B) External absorbed dose rate (µGy.h^{-1})

Soil sample	External absorbed dose rate (µGy.h^{-1})											
	^{137}Cs		^{90}Sr		^{241}Am		^{60}Co		^{154}Eu		^{234}U	
	Apr 09	Oct 09	Apr 09	Oct 09	Apr 09	Oct 09	Apr 09	Oct 09	Apr 09	Oct 09	Apr 09	Oct 09
1	1.69E+01	1.69E+01	1.32E+01	1.32E+01	8.41E+01	1.36E+02	1.24E-02	1.24E-02	7.45E-02	1.19E-01	3.11E+02	2.89E+02
3	1.21E+01	3.02E+01	9.45E+00	2.36E+01	6.01E+01	1.68E+02	8.88E-03	2.63E-02	5.32E-02	1.19E-01	1.12E+02	5.16E+02
4	2.46E+00	5.64E+00	1.92E+00	4.41E+00	1.22E+01	2.40E+01	1.81E-03	2.26E-03	1.08E-02	1.98E-02	4.72E+01	9.63E+01
8	2.58E+01	2.70E+01	2.01E+01	2.11E+01	1.28E+02	9.98E+01	1.89E-02	1.53E-02	1.13E-01	1.02E-01	4.69E+02	4.61E+02
10	1.17E+01	2.86E+01	9.13E+00	2.24E+01	5.81E+01	1.28E+02	8.58E-03	2.10E-02	5.14E-02	1.42E-01	1.99E+02	4.88E+02
12	1.05E+01	1.49E+01	8.19E+00	1.16E+01	5.21E+01	7.19E+01	7.70E-03	1.17E-02	4.61E-02	4.53E-02	1.79E+02	2.54E+02
13	1.49E-02	6.04E-02	1.16E-02	4.72E-02	7.41E-02	3.00E-01	1.10E-05	4.44E-05	6.56E-05	2.66E-04	2.54E-01	1.03E+00
14	3.67E-02	3.18E-02	2.87E-02	2.49E-02	1.82E-01	1.58E-01	2.69E-05	2.34E-05	1.61E-04	1.40E-04	6.26E-01	5.43E-01
20	1.41E-02	2.18E-02	1.10E-02	1.70E-02	7.01E-02	1.08E-01	1.04E-05	1.60E-05	6.21E-05	9.57E-05	2.41E-01	3.71E-01

Soil sample	External absorbed dose rate (µGy.h^{-1})											
	^{235}U		^{236}U		^{232}Th		^{239}Pu		^{240}Pu		^{241}Pu	
	Apr 09	Oct 09	Apr 09	Oct 09	Apr 09	Oct 09	Apr 09	Oct 09	Apr 09	Oct 09	Apr 09	Oct 09
1	7.75E+00	7.19E+00	2.88E+01	2.49E+01	2.11E+01	2.13E+01	3.29E+04	3.30E+04	4.70E+04	4.93E+04	1.48E+02	1.42E+02
3	2.88E+00	1.28E+01	9.63E+00	4.45E+01	2.39E+01	2.13E+01	1.08E+04	5.89E+04	1.59E+04	8.81E+04	4.69E+01	2.53E+02
4	1.44E+00	2.40E+00	3.07E+00	8.30E+00	1.97E+01	2.13E+01	3.40E+03	1.10E+04	5.23E+03	1.64E+04	1.69E+01	4.72E+01
8	1.25E+01	1.15E+01	3.93E+01	3.97E+01	2.26E+01	2.13E+01	5.40E+04	5.27E+04	7.78E+04	7.87E+04	2.00E+02	2.26E+02
10	3.28E+00	1.21E+01	1.72E+01	4.21E+01	2.31E+01	2.13E+01	3.02E+04	5.58E+04	5.56E+04	8.34E+04	1.98E+02	2.39E+02
12	3.98E+00	6.33E+00	1.54E+01	2.19E+01	2.00E+01	2.13E+01	1.83E+04	2.91E+04	2.68E+04	4.35E+04	6.83E+01	1.25E+02
13	4.44E-01	2.57E-02	2.19E-02	8.89E-02	1.96E+01	2.13E+01	2.91E+01	1.18E+02	4.35E+01	1.76E+02	1.25E-01	5.06E-01
14	4.66E-01	1.35E-02	5.40E-02	4.68E-02	1.71E+01	2.13E+01	6.63E+01	6.21E+01	2.88E+02	9.28E+01	6.07E-01	2.66E-01
20	4.99E-01	9.24E-03	3.49E-02	3.20E-02	2.44E+01	2.13E+01	2.75E+01	4.24E+01	1.68E+02	6.34E+01	1.78E+00	1.82E-01

Table S4 : taxonomic affiliation and distribution of OTUs with (*i*) a relative abundance significantly different between the trench and the surrounding soils and (*ii*) with >1% abundance in at least one soil sample. The trench soil samples and specific OTUs are highlighted in red. The surrounding soil samples and specific OTUs are highlighted in blue.

#OTU ID	taxonomy	1A	1O	3A	3O	4A	4O	8A	8O	10A	10O	12A	12O	13A	13O	14A	14O	20A	20O
1143180	Archaea;Crenarchaeota;Thaumarchaeota;Cenarchaeales;SAGMA-X	7.30	2.07	0.31	1.05	0.77	0.31	1.90	1.02	2.58	4.90	0.12	1.77	0.04	0.01	0.00	0.14	0.09	0.08
nrOTU63	Bacteria;Acidobacteria;[Chloracidobacteria];11-24	0.00	0.11	0.04	0.01	0.06	0.32	5.16	0.50	0.03	1.03	0.17	0.48	0.00	0.00	0.01	0.00	0.05	0.02
219830	Bacteria;AD3;ABS-6	2.01	0.42	1.12	0.78	1.47	2.36	4.07	4.65	3.48	3.37	2.48	3.18	1.15	0.37	0.10	0.20	0.36	0.28
204059	Bacteria;AD3;ABS-6	0.89	0.42	1.90	0.34	0.09	0.43	0.86	1.50	3.62	0.32	1.94	3.87	0.12	0.02	0.96	0.08	1.10	0.47
125947	Bacteria;Proteobacteria;Betaproteobacteria;Burkholderiales;Burkholderiaceae;Burkholderia	0.04	0.01	0.03	0.09	0.01	0.02	0.00	3.43	0.00	0.06	0.33	0.01	0.07	0.00	0.02	0.02	0.01	0.00
161623	Bacteria;AD3;JG37-AG-4	3.21	1.47	0.94	0.27	1.27	1.59	1.31	1.05	1.68	1.85	1.02	0.95	0.29	0.07	0.26	0.98	0.48	0.24
573135	Bacteria;Proteobacteria;Alphaproteobacteria;Rhizobiales;Bradyrhizobiaceae;Bradyrhizobium	0.38	0.33	0.23	2.90	0.44	0.19	0.08	0.43	0.10	0.26	0.60	0.32	0.10	0.02	0.65	0.25	0.26	0.15
658707	Bacteria;Verrucomicrobia;[Pedosphaerae];[Pedosphaerales];auto67_4W	1.71	0.25	0.01	0.00	0.00	0.00	2.32	0.29	0.55	0.70	0.91	0.02	0.00	0.00	0.00	0.00	0.00	0.00
4424841	Bacteria;WPS-2	0.01	0.01	0.03	2.22	0.02	0.14	0.20	0.35	0.44	0.42	0.16	1.03	0.34	0.00	0.00	0.00	0.05	0.01
4383662	Bacteria;Planctomycetes;Planctomycetia;Gemmatales;Gemmataceae	1.34	0.80	0.85	0.20	1.52	2.22	1.95	0.84	0.90	0.43	0.36	0.68	0.13	0.00	0.08	0.38	0.32	0.43
3117367	Bacteria;Chloroflexi;Ktedonobacteria;Ktedonobacterales;Ktedonobacteraceae	0.26	0.21	0.09	1.93	0.31	0.19	0.19	0.29	0.25	0.61	0.20	0.40	0.03	0.00	0.00	0.00	0.07	0.00
154822	Bacteria;Acidobacteria;DA052;Ellin6513	0.20	0.60	0.75	0.37	0.70	1.05	0.46	1.69	1.39	0.80	0.91	1.44	0.07	0.03	0.05	0.37	0.41	0.35
1123749	Bacteria;WPS-2	0.44	0.68	0.38	0.08	0.53	0.46	1.52	1.02	0.83	1.51	1.35	0.55	0.13	0.05	0.01	0.15	0.10	0.04
209467	Bacteria;Acidobacteria;iii1-8;DS-18	1.49	1.01	0.03	0.01	0.62	0.40	0.83	0.59	0.06	0.03	0.03	0.14	0.17	0.00	0.00	0.00	0.03	0.09
153350	Bacteria;Acidobacteria;DA052;Ellin6513	0.40	0.10	0.05	0.01	0.08	0.40	0.69	0.20	1.16	1.43	0.03	0.17	0.00	0.00	0.00	0.00	0.00	0.00
4342107	Bacteria;Proteobacteria;Alphaproteobacteria;Rhizobiales;Hyphomicrobiaceae;Rhodoplanes	0.63	0.62	1.12	0.29	0.96	1.19	0.40	0.60	0.44	0.31	1.30	1.10	0.07	0.04	0.05	0.46	0.57	0.46
78839	Bacteria;Acidobacteria;DA052;Ellin6513	0.83	0.41	0.23	0.61	0.18	0.28	0.97	0.72	0.81	1.29	1.15	0.61	0.03	0.05	0.04	0.35	1.17	0.37
1121144	Bacteria;Proteobacteria;Gammaproteobacteria;Xanthomonadales;Sinobacteraceae	0.29	1.07	0.16	0.22	0.05	0.41	0.73	0.65	0.13	0.44	0.26	0.62	0.07	0.08	0.31	0.11	0.57	0.50
113331	Bacteria;Acidobacteria;DA052;Ellin6513	0.40	0.19	0.03	0.03	0.11	0.13	1.01	0.70	0.50	1.00	0.12	0.41	0.01	0.00	0.00	0.03	0.02	0.00
223820	Bacteria;AD3;ABS-6	0.30	0.43	3.30	0.46	0.55	3.18	0.42	0.73	2.08	0.37	1.11	0.98	9.84	17.07	3.18	3.83	4.24	5.35
254530	Bacteria;Verrucomicrobia;[Spartobacteria];[Chthoniobacterales];[Chthoniobacteraceae];DA101	0.09	0.36	2.85	0.28	1.44	1.91	0.05	0.12	0.08	0.04	0.14	0.09	7.70	10.88	4.04	5.55	1.65	1.99
278511	Bacteria;Acidobacteria;DA052;Ellin6513	0.02	0.05	0.04	0.02	0.03	0.08	0.02	0.03	0.01	0.02	0.04	0.02	0.00	0.00	8.07	0.01	0.03	0.01
205773	Bacteria;AD3;ABS-6	0.47	0.45	2.62	0.64	0.54	0.87	0.72	1.01	4.03	0.31	1.85	2.05	5.25	5.92	0.47	1.59	3.97	3.62
220148	Bacteria;AD3;JG37-AG-4	0.07	0.06	1.27	0.30	1.47	3.07	0.04	0.14	0.82	0.12	0.15	0.35	0.67	1.95	5.89	3.52	0.88	1.35
nrOTU78	Bacteria;AD3;JG37-AG-4	0.00	0.00	0.49	0.02	0.01	0.30	0.00	0.04	0.17	0.00	0.05	0.07	3.88	4.96	2.32	3.14	0.90	1.28
nrOTU44	Bacteria;AD3;JG37-AG-4	0.12	0.06	1.98	0.47	2.06	1.24	0.77	0.58	0.77	0.37	0.58	2.40	2.56	3.52	1.38	2.25	1.07	1.26
248375	Bacteria;Actinobacteria;MB-A2-108	0.00	0.00	0.06	0.03	0.00	0.00	0.00	0.00	0.00	0.01	0.12	0.03	1.48	3.18	1.48	2.01	0.35	2.90
811458	Bacteria;AD3;JG37-AG-4	0.05	0.03	1.12	0.49	0.80	1.99	0.04	0.12	0.88	0.04	0.18	0.39	2.00	1.60	0.94	1.62	1.87	3.11
2984011	Bacteria;Gemmatimonadetes;Gemm-1	0.02	0.00	0.17	0.03	0.03	0.00	0.00	0.00	0.00	0.00	0.01	0.01	0.27	0.61	3.07	0.38	0.17	0.35
205456	Bacteria;Verrucomicrobia;[Spartobacteria];[Chthoniobacterales];[Chthoniobacteraceae];DA101	0.05	0.39	0.60	0.44	0.10	0.20	0.01	0.26	0.00	0.01	0.59	0.10	1.13	0.55	0.64	2.24	3.01	2.95
4448095	Bacteria;Actinobacteria;Actinobacteria;Actinomycetales;Mycobacteriaceae;Mycobacterium	0.01	0.08	0.08	0.14	0.00	0.02	0.05	0.19	0.22	0.02	0.35	0.09	0.30	0.78	2.87	0.15	0.10	0.27
207672	Bacteria;Acidobacteria;iii1-8;DS-18	0.00	0.00	0.14	0.02	0.01	0.04	0.00	0.00	0.00	0.00	0.04	0.00	0.27	0.42	2.65	0.71	0.73	1.01
3587027	Bacteria;Acidobacteria;iii1-8;32-20	0.00	0.00	0.08	0.00	0.02	0.02	0.00	0.00	0.00	0.00	0.04	0.00	2.50	1.51	1.36	0.08	0.70	2.17
4474277	Archaea;Crenarchaeota;MBGA;NRP-J	0.00	0.00	0.00	0.00	0.00	0.00	0.00	0.00	0.06	0.00	0.08	0.16	1.11	2.11	0.13	0.07	0.98	1.18
821237	Bacteria;Verrucomicrobia;[Spartobacteria];[Chthoniobacterales];[Chthoniobacteraceae];DA101	0.03	0.16	1.05	0.16	0.16	0.25	0.02	0.10	0.04	0.01	0.05	0.04	2.03	1.49	1.18	0.91	1.04	1.01
4470401	Bacteria;AD3;ABS-6	1.07	0.24	0.53	0.46	0.49	0.14	0.37	0.51	1.79	0.22	1.26	1.10	0.61	0.99	0.23	1.86	1.06	0.59
nreOTU22	Bacteria	0.00	0.00	0.01	0.00	0.00	0.00	0.01	0.04	0.06	0.00	0.09	0.07	0.02	0.13	0.79	1.60	0.42	0.74
ncurOTU10624	Bacteria	0.00	0.00	0.00	0.00	0.00	0.00	0.00	0.00	0.00	0.00	0.02	0.05	1.55	1.51	0.67	1.44	0.03	0.15
1144253	Bacteria;WPS-2	0.00	0.00	0.11	0.04	0.08	0.27	0.20	0.19	0.54	0.15	0.43	0.38	0.85	1.20	0.29	0.37	0.92	0.47

Table S5: major OTUs being more abundant in the trench than in the surrounding soils and a selection of their closest neighbours in the nr database. A colour code is used to highlight particular features of the environment from which the sequences are derived: radionuclides/radioactivity/heavy metal in red; volcanic/fire in green, cold in blue and acid in yellow.

OTU ID	Taxonomy	Closest relatives	identity	Origin
1143180	Archaea;Crenarchaeota;Thaumarchaeota;Cenarchaeales;SAGMA-X	AB050208	100%	acid water from gold mines, South Africa
OTUnr63	Bacteria;Acidobacteria;[Chloracidobacteria];11-24	KP915812	99%	soil after volcanic eruption on Kasatochi Island, Alaska
209467	Bacteria;Acidobacteria;iii1-8;DS-18	KF974114	99%	permafrost-affected soils of Northeast Greenland
153350	Bacteria;Acidobacteria;DA052;Ellin6513	EF221418	99%	Antarctic terrestrial habitats
		HQ322990	98%	acid mine drainage in a long abandoned mining site
		FJ570382	98%	alpine tundra soils
		GU393466	98%	anoxic neptunium-containing sediments
154822	Bacteria;Acidobacteria;DA052;Ellin6513	JF300958	100%	boreal forest soil
		EU849210	100%	acidic subalpine forest and fire-induced grassland,Taiwan
		FJ625362	100%	lead contamination of boreal pine forest
78839	Bacteria;Acidobacteria;DA052;Ellin6513	AJ536864	100%	soil samples of uranium wastes
		DQ450707	99%	alpine tundra wet meadow soil
		GU393453	99%	anoxic neptunium-containing sediments
		GU047460	99%	active layer and permafrost in an acidic wetland, Arctic
		FJ466151	99%	Hawaiian volcanic deposit
		FJ570548	99%	alpine tundra soils
		GQ287472	99%	Pindari glacier, Himalayan mountain ranges, India
113331	Bacteria;Acidobacteria;DA052;Ellin6513	KP905379	100%	soil after volcanic eruption on Kasatochi Island, Alaska
219830	Bacteria;AD3;ABS-6	KP906936	100%	soil after volcanic eruption on Kasatochi Island, Alaska
		FJ570325	100%	alpine tundra soils
		HM065752	99%	Dama glacier, Switzerland
204059	Bacteria;AD3;ABS-6	JF833936	100%	potassium mine soil, China
		AB821068	100%	lava forest soil, Korea
161623	Bacteria;AD3;JG37-AG-4	JX869474	100%	acid sulfate soil, Finland
		DQ450737	100%	alpine tundra wet meadow soil
		KP906130	100%	soil after volcanic eruption on Kasatochi Island, Alaska
		HG324327	100%	cellulose degradation in acidic fen soil
		FJ625337	100%	lead contamination of boreal pine forest
573135	Bacteria;Proteobacteria;Alphaproteobacteria;Rhizobiales;Bradyrhizobiaceae;Bradyrhizobium	LT617088	100%	dust samples from the Russian part of the ISS
4304723	Bacteria;Proteobacteria;Betaproteobacteria;SC-I-84	GU393494	100%	anoxic neptunium-containing sediments
1121144	Bacteria;Proteobacteria;Gammaproteobacteria; Xanthomonadales;Sinobacteraceae	KT018626	100%	Cr(VI)-contaminated Soils
		KF800867	100%	Himalayan Mountains
658707	Bacteria;Verrucomicrobia;[Pedosphaerae];[Pedosphaerales]; auto67_4W	KU221979	99%	Hengill Valley, Iceland
		AB364854	99%	boreal oligotrophic peat wetlands
		FJ466366	99%	Hawaiian volcanic deposit
		KF863914	99%	acidic soil near an acid mine drainage, China
4424841	Bacteria;WPS-2	GQ329594	100%	Pindari glacier, Himalayan mountain ranges
1123749	Bacteria;WPS-2	KC562917	100%	soil, Sergyemla Mountains, southeast Tibet
		GU393463	100%	anoxic neptunium-containing sediments
		FJ570155	100%	alpine tundra soils
		EU421867	100%	Lahaul-Spiti Valley of The Indian Himalayas
		KP905215	100%	soil after volcanic eruption on Kasatochi Island, Alaska

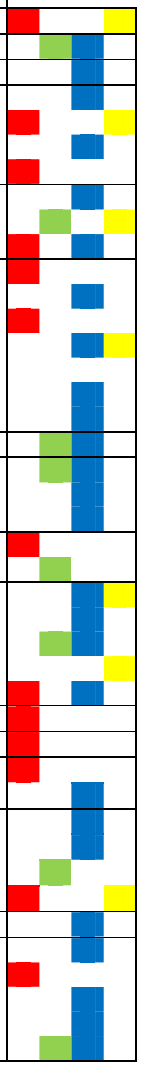

Table S6:distribution and taxonomic affiliation of the 5 most abundant OTUs having a cultured representative. The OTUs specific of the trench are highlighted in red.

OTU ID	1A	1O	3A	3O	4A	4O	8A	8O	10A	10O	12A	12O	13A	13O	14A	14O	20A	20O	taxonomic affiliation
4057260	0.06	0.01	0.26	6.97	0.00	0.01	0.01	0.01	0.24	0.73	0.57	1.28	0.00	0.00	0.66	0.00	0.33	0.41	Proteobacteria;Betaproteobacteria;Burkholderiales;Burkholderiaceae;Burkholderia
125947	0.04	0.01	0.03	0.09	0.01	0.02	0.01	3.43	0.00	0.06	0.33	0.01	0.07	0.00	0.02	0.02	0.01	0.00	Proteobacteria;Betaproteobacteria;Burkholderiales;Burkholderiaceae;Burkholderia
573135	0.38	0.33	0.23	2.90	0.44	0.20	0.08	0.44	0.10	0.26	0.60	0.32	0.11	0.02	0.65	0.25	0.26	0.15	Proteobacteria;Alphaproteobacteria;Rhizobiales;Bradyrhizobiaceae;Bradyrhizobium
156722	0.00	0.00	0.02	0.05	0.00	0.00	0.00	0.08	0.04	0.04	0.25	0.07	0.01	0.00	0.77	0.36	0.12	0.21	Proteobacteria;Betaproteobacteria;Burkholderiales;Burkholderiaceae;Burkholderia
196652	0.03	0.00	0.62	0.21	0.00	0.00	0.00	0.27	0.06	0.71	0.13	0.04	0.02	0.00	0.05	0.17	0.02	0.05	Proteobacteria;Betaproteobacteria;Burkholderiales;Burkholderiaceae;Burkholderia